REMOTELY SENSED PROXIES FOR GROSS PRIMARY PRODUCTION AT DIFFERENT TIME-SCALES

SHORT TERM SCIENTIFIC MISSION (STSM)

Applicant- João Pedro Carreira, Universidade de Aveiro, Aveiro, Portugal (PT)

Hosts–Dr. Nuno Carvalhais and Dr. Mirco Migliavacca

Department Biogeochemical Integration at the

Max-Plank Institute for Biogeochemistry, Jena (DE)

COST STSM Reference Number: COST-STSM-ES1309-36114

COST Action: ES1309

Contents

1. PURPOSE OF THE STSM

The STSM's overarching aim was to contribute to the integration of data on spectral reflectance with data on ecosystem productivity across temporal scales, bycombining ground, tower and satellite measurements. The training opportunity thus aimed at exploring the links between remotely sensed data (such as the NDVI, EVI, LAI, FPAR, fluorescence) and gross primary production retrieved at several FLUXNET eddy covariance (EC) sites (D. Baldocchi, 2008; D. D. Baldocchi, 2003) at different temporal scales, from seasonal to interannual variability. The current research focused strongly on a Canadian post-fire chronosequence which builds on the proposed goals by integrating a longer term component to the analysis, but spatially circumscribed to the set of six EC sites. Such chronosequences allows further investigation of the impacts of stand replacement fire disturbances on the vegetation recovery and consequent responses in the ecosystem carbon fluxes. These goals provide strong links between OPTIMISE, and the candidate's PhD study, as well as to the EU-FP7 project CASCADE and the national project FIRE-C-BUDs, which aim at investigating vegetation and ecosystem recovery dynamics in Mediterranean ecosystems that are highly fire-prone.

2. DESCRIPTION OF THE WORK CARRIED OUT DURING THE STSM

2.1 RESEARCH QUESTIONS

The STSM addressed the following research questions

a) Which remotely sensed based vegetation indexes relate best to GPP (gross primary production) estimates at different time scales (annual, seasonal, monthly)?
b) Which methods and techniques for treatment of VIs time series are best suited to analyze the links between Vis with GPP?
c) How do the different VIs translate the post-fire recovery dynamics? Which VIs are more linked to the long term recovery C-fluxes?

2.2 DATA

2.2.1 TOWER DATA

Several sites in Canada with freely-available EC tower data were selected to obtain a chronosequence of time-since-fire (**Table 1**) (Goulden et al., 2006). For each of the towers, the data on GPP, radiation, vapor pressure deficit, temperature daily data were retrieved when available, over a roughly 15 year period, starting at the beginning of 2000 and ending at the beginning of 2015. As an example, GPP data for the CA-NS2 site roughly cover a three year period: 2001, 2002, 2003.

TABLE 1 - RESEARCHED FLUXNET TOWERS

Tower code	Location	Vegetation IGBP	Time-since-fire (years)
CA-NS2	Canada	Evergreen Needleleaf Forests	87
CA-NS3	Canada	Evergreen Needleleaf Forests	53
CA-NS4	Canada	Evergreen Needleleaf Forests	53
CA-NS5	Canada	Evergreen Needleleaf Forests	36
CA-NS6	Canada	Evergreen Needleleaf Forests	28
CA-NS7	Canada	Evergreen Needleleaf Forests	19

The chronosequence presented was used for methodological and conceptual purposes, specially relating to research question c). The consequential chronosequence analysis can further be extended in the near future to other chronosequence sites

2.2.2 SATELLITE DATA

Over that same time period (2000 to 2015), several VIs (vegetation indexes) from MODIS (FPAR, LAI, NDVI, EVI) and GOME-2 (fluorescence) remote sensing products were retrieved for all tower locations:

- FPAR (Fraction of Photosynthetically Active Radiation,) 8 day composite, 1 Km product (Knyazikhin, Martonchik, Diner, et al., 1998; Knyazikhin, Martonchik, Myneni, Diner, & Running, 1998)
- LAI (Leaf Area Index,) 8 day composite, 1 Km product (Knyazikhin, Martonchik, Diner, et al., 1998; Knyazikhin, Martonchik, Myneni, et al., 1998)
- NDVI (Normalized Difference Vegetation Index), 16 day composite, 250 m product (Huete, 1997; Huete et al., 2002; Justice et al., 2002; Rouse, Hass, Schell, & Deering, 1974)
- EVI (Enhanced Vegetation Index), 16 day composite, 250 m product (Huete et al., 2002; Justice et al., 2002)
- GOME-2 fluorescence monthly,0.5º product (Joiner et al., 2013)

Unfortunately, GOME-2 fluorescence data could not be included in the posterior analysis as they do not overlap in time with the GPP data sets. GOME-2 fluorescence data might be used for future research with other sites, where convenient.

2.3 STATISTICAL ANALYSIS

For each of the MODIS VIs – FPAR, LAI, EVI and NDVI – the original time series was retrieved and then processed using various methods designed to gapfill and correct for underestimation biases the original series, listed in **Table 2**. This resulted in 26 data sets for each of the four MODIS variables, one of which being the original time series. At first, all VIs subjected to the different treatments were cross-compared between them, resulting in a 108x 108correlation matrix.

Further, correlation analysis supported the comparisons between the sites' remote sensing VIs at different temporal aggregation and the EC GPP retrievals. This was done over several temporal aggregations, namely annual, seasonal (spring, summer, autumn, winter) and monthly (each of the twelve months). Data retrieved from the towers was subjected to quality control filter, only considering: (i) daily values resulting from half hourly aggregations comprising more that 80% of good or very good quality records quality above 0.8; and (ii) when data availability covered at least 75% of the total aggregation period. This assured that data was of good quality and that there were enough valid records to be representative of a specific temporal aggregation.

The temporal aggregations for the MODIS and EC data sets considered three different metrics: the mean and the 50 and 90 percentiles. Overall, 324 MODIS based time series (4 VIs x 28 methods x 3 aggregation metrics) were compared with each of the three GPP aggregations at an annual, seasonal as well as monthly time scale.

TABLE 2 - METHODS AND BRIEF DESCRIPTION

Methods	Description
Original	Original time series (may contain data with poor quality)
fitAG, fitDL, fitSG, fitMD	time series fit of timesat (Chen et al., 2004; Jönsson & Eklundh, 2004)
corAG,corDL, corSG, corMD	time series correction with timesat (Chen et al., 2004; Jönsson & Eklundh, 2004)
corFFT1,corFFT2, corBISE1,corBISE2	fast fourier transformation (approximation) (Carvalhais et al., 2008; Sellers et al., 1996; Viovy, Arino, & Belward, 1992)
corFFT1_spatialgapsMean, corFFT2_spatialgapsMean, corBISE1_spatialgapsMean, corBISE2_spatialgapsMean	corrected with mean of the gap filled neighbors
corFFT1_spatialgaps, corFFT2_spatialgaps, corBISE1_spatialgaps, corBISE2_spatialgaps	corrected with time series of the gap filled neighbors that are best correlated with the center pixel
MSC, Reg, RegMSC	correct with mean seasonal cycle, best correlated neighbors and both
ens_P50, ens_AVG	ensemble P50 and average of all methods above

3. DESCRIPTION OF THE MAIN RESULTS OBTAINED

3.1 REMOTELY SENSED VIS FOR GROSS PRIMARY PRODUCTION AT DIFFERENT TIME-SCALES (RESEARCH QUESTIONS A AND B)

The correlation matrix of all the VI-methods against the same VI-methods (order is FPAR, LAI, EVI, NDVI) of the CA-NS3 MODIS data is shown in **Figure 1**, suggesting basically that the FPAR, LAI and NDVI are generally more closely-related than with the EVI. The low correlation between EVI was observed at all sites in this chronosequences, which was very unexpected given the relationship between NDVI and EVI (e.g.Huete et al., 2002). A further investigation revealed that the EVI data time series for the Canadian sites was contaminated with a high level of noise (annex A **Figure 12**). In annex B, **Figure 13** , we have added a correlation matrix from another EC site (PT-Mi1 Portugal, Évora) in which the EVI appears to have the expected seasonal behavior. However, for this chronosequences sites we found no reason behind this abnormal behavior in EVI, but since it did not portrait the typical Canadian vegetation seasonality, we removed the EVI from any posterior analysis in this exercise. Additionally there is a clear pattern that reflect that the NDVI in general compared both to LAI and FPAR, but that for the LAI-FPAR relationship some methods correlate worst (CorFFT2, corFFT_spacialgapsMean, corFFT2_spatialgapsMean, corFFT1_spatialgaps, corFFT2_spatialgaps). The best correlations across VI's (except EVI) were found for REgMSC, MSC, Reg.

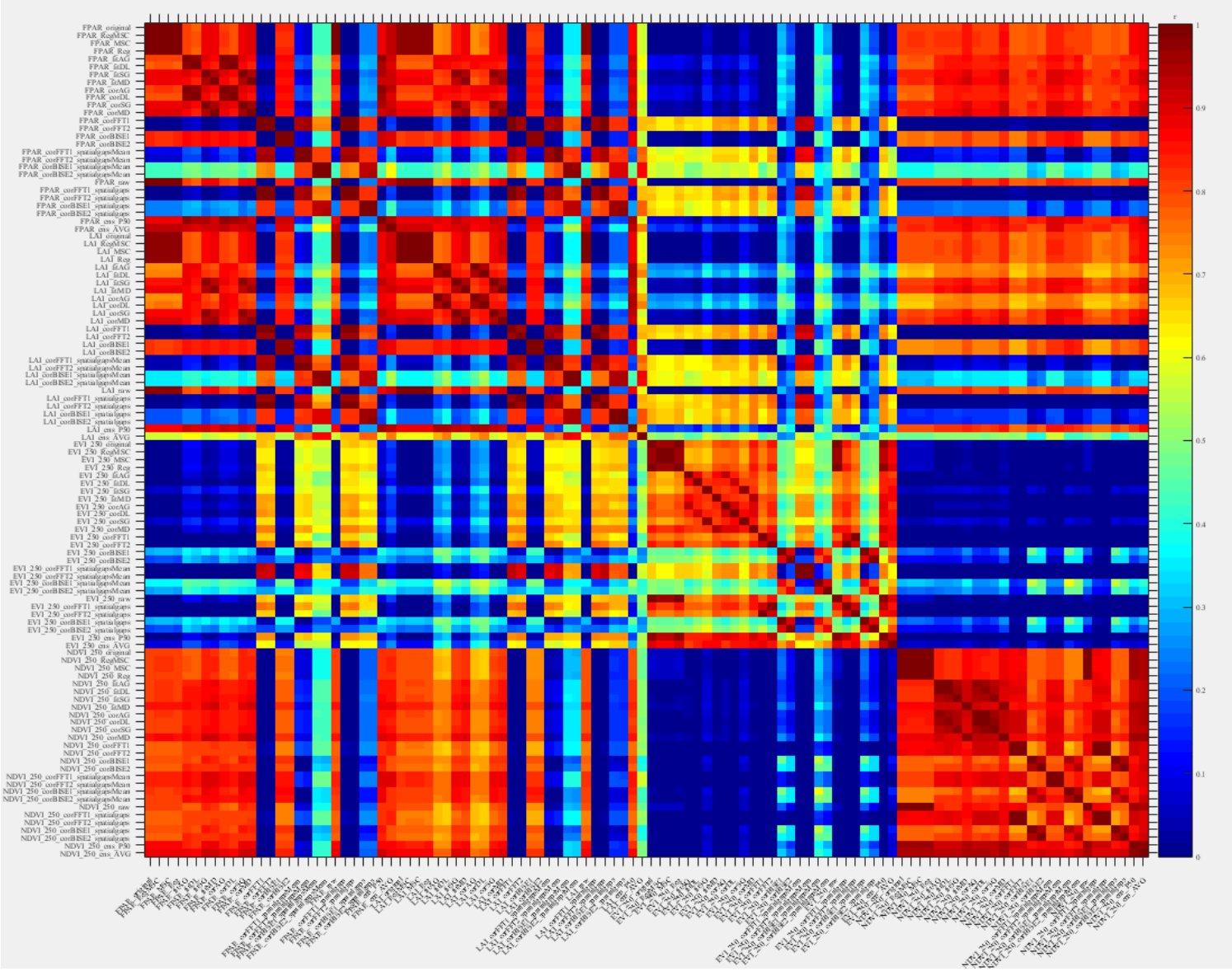

FIGURE 1 - CORRELATION MATRIX OF VI-METHODS AGAINST VI-METHODS

The different aggregation methods (mean, P50 and P90) and VIs time series were then analyzed for the Canadian sites and correlated with EC GPP. This resulted in 17 different correlation matrixes (1 annual, 4 seasonal and 12 monthly) of 3 (mean, P50, P90 - GPP) x 324 proxies (mean, P50, P90 – VI-methods). Correlations were done from all sites and all times available, so that they include not only temporal but also spatial variation. An illustration of annual correlations is shown in **Figure 2**.

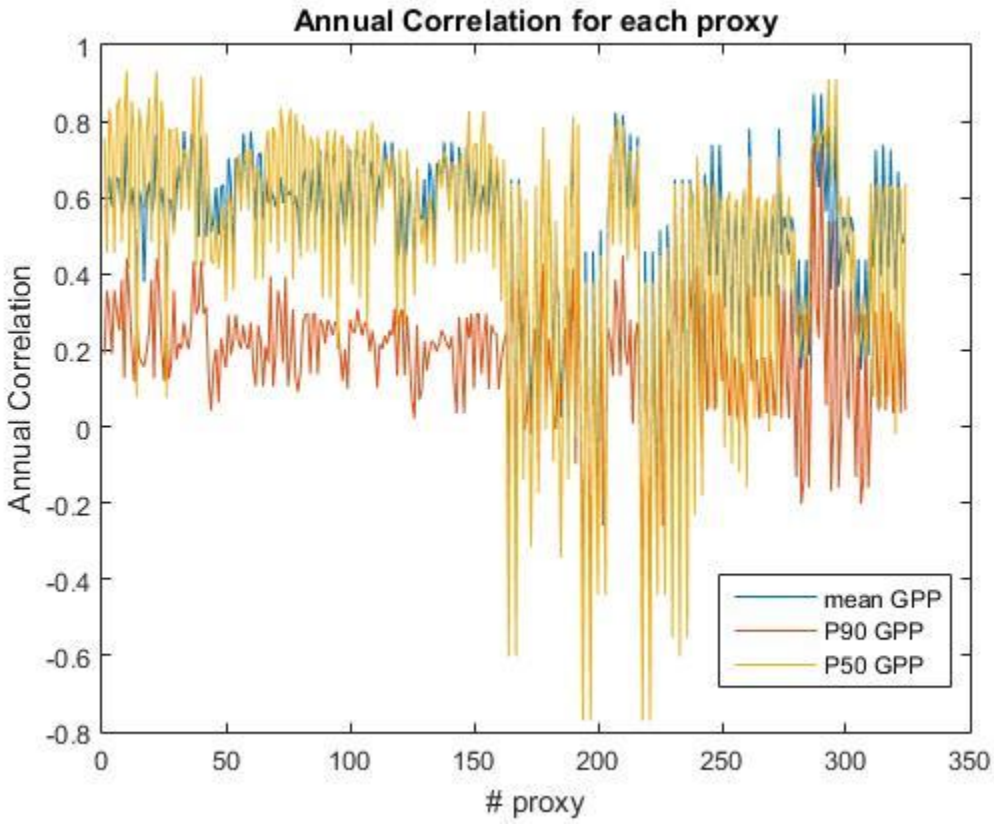

FIGURE 2-ANNUAL CORRELATIONS FOR EACH PROXY

Figure 2 shows that mean and P50 GPP estimates tend to correlate better with mean and P50 proxies than P90 GPP estimates. The figure also shows an area of strongly negative (not expected correlations) which are related to the noisy EVI (which results should not be considered). Similar figures can be devised for seasonal and monthly correlations. Nevertheless, from inspection of the correlation matrix, strong correlations were found in spring and April/May (**Figure 3, 4 and 5**). Despite the fact that peak plant growth occurs mainly in the summer period in these sites, the finding that May proxies might be used to estimate annual GPP mean or P50 values suggests that the inter annual variability (IAV) in GPP is strongly linked to the beginning of the growing season. Another hypothesis, that was not tested, is that IAV is mostly controlled by the length of growing season, which would be varying according to the beginning of the growing season if end of season dates would not change substantially.

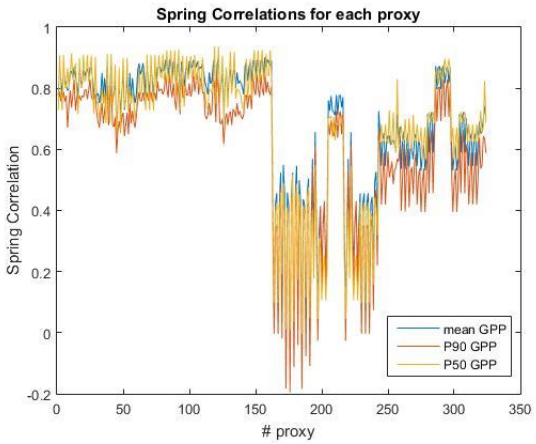

FIGURE 3 - SPRING CORRELATIONS FOR EACH PROXY

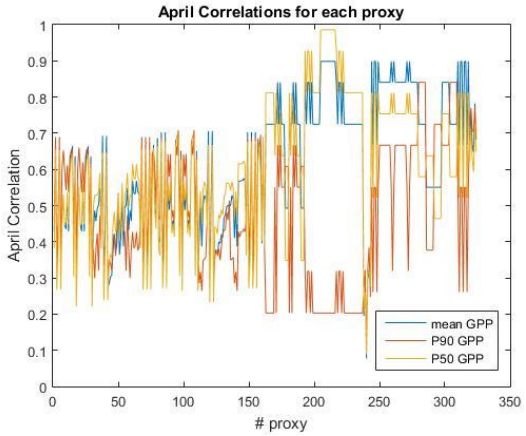

FIGURE 4 - APRIL CORRELATIONS FOR EACH PROXY

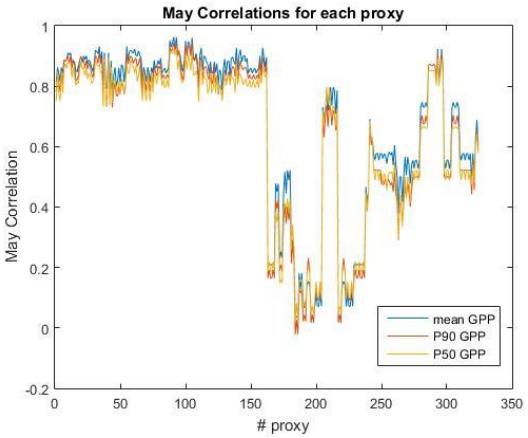

FIGURE 5 - MAY CORRELATIONS FOR EACH PROXY

Concluding:

(i)**Figures 2, 3, 4 and 5** clearly exhibit a different EVI pattern (proxies 163-243) consistent to a poor signal quality. This reinforces the choice to remove the EVI from the analysis;

(ii) Apparently FPAR (proxies 1-81) and LAI (proxies 82-162) are more robust to act as proxies for GPP. Additionally, given the stable values of high correlations within this proxies zones, that might be more important than the method of correction used. This will be further tested with an Anova (**see section 4**);

(iii) Knowledge of spring VI is very important for understanding interannual variability.

3.2 Recovery Dynamics (research Question c)

Towards the fire chronosequence analysis, several approaches were tested being that FPAR against stand age (in relation to their last fire disturbance) provided an interesting insight that is presented on **figure 6**.

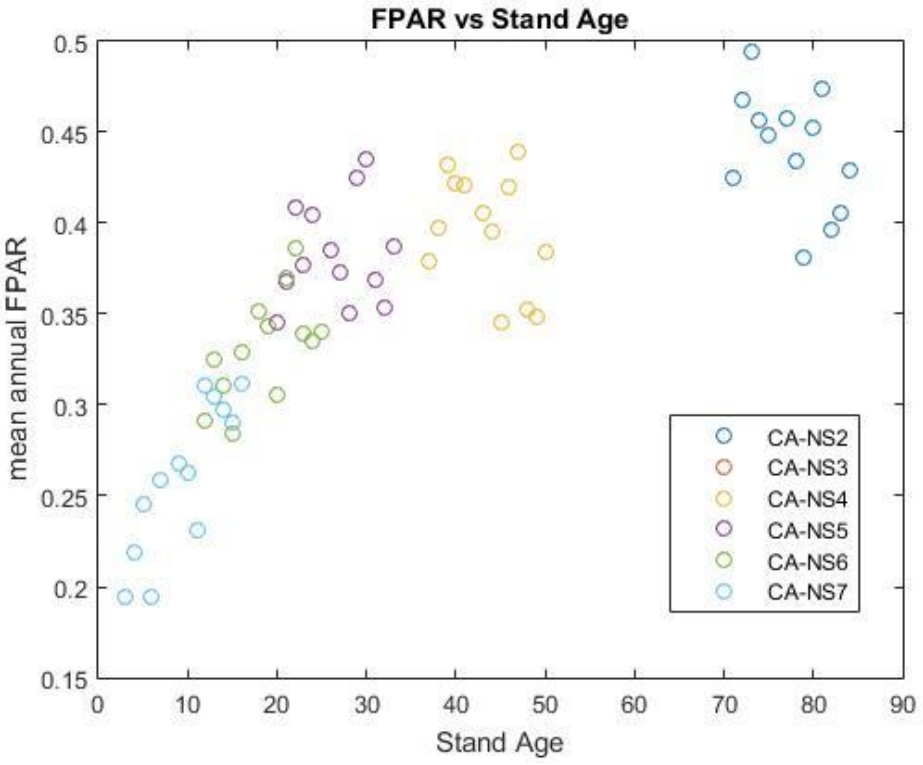

FIGURE 6 - FPAR (MEAN ANNUAL ORIGINAL VALUES) VS AGE OF STANDS

This result could be interpreted as that the fraction of photosynthetic absorbed radiation at the sites increases approximately linearly with time up to 30 years reaching an FPAR of 0.45, after which it tends to moderately increase up to a maximum of 0.5, as the age of the site is getting older. This presents an interesting overview of vegetation recovery, as that CA-NS6 and CA-NS7 sites are still represented by young forest stages, so we can possibly see an evolution to mature forest environments. This relation becomes also evident with the LAI (**figure 7**).

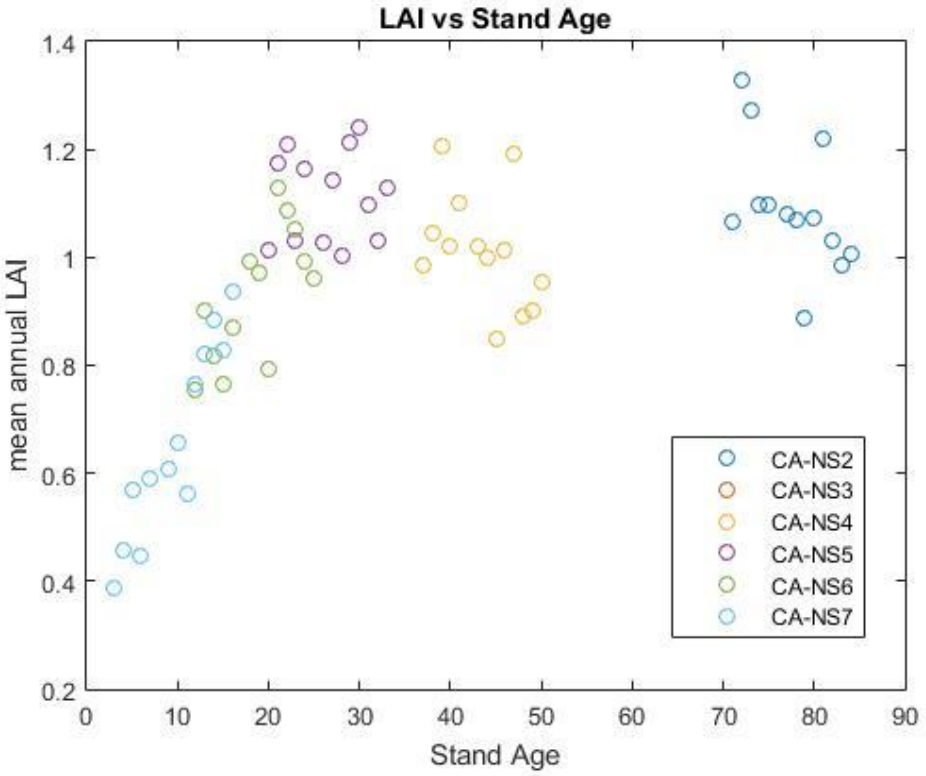

FIGURE 7 - LAI (MEAN ANNUAL ORIGINAL VALUES) VS STAND AGE

Mean annual LAI recovery trajectory reflects that the forest have reach the coverage at maturity around 20-30 years after disturbance (Chasmer et al., 2008), only modestly increasing up to 90 years. However, a different type of result is shown in **Figure 8**, where the temporal aggregation used was the LAI annual percentile 90 instead of the mean.

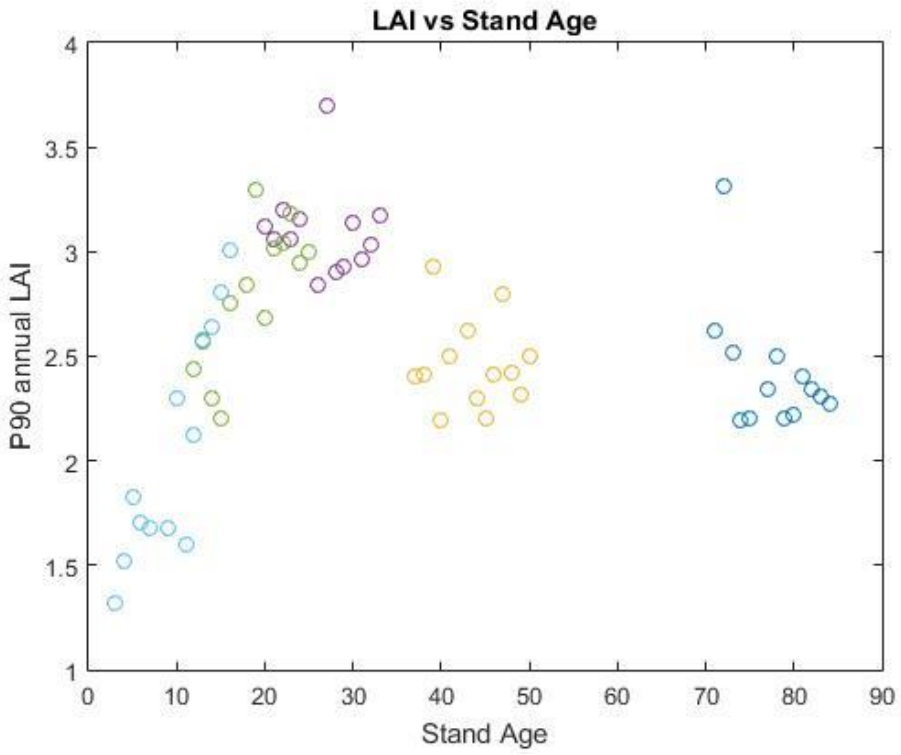

FIGURE 8 - LAI (P90 ANNUAL ORIGINAL VALUES) VS STAND AGE

Figure 8 shows that the peak leaf area coverage occurs around 20 to 30 years being that as the forest matures the leaf coverage stabilizes and slightly diminishes. However, this reduction in LAI above 30 years is not obvious in the mean LAI values (**Figure 7**). Serbin (2013) concluded that "MODIS LAI and FPAR products overestimated and underestimated the LAI and FPAR for the youngest and oldest sites, respectively", which could suggest a stronger difference in LAI and FPAR between young and older sites and also could explain the later successional reductions in LAI seen in **figures 7 and 8**.

When the NDVI is plotted against stand age a different type of result is presented (**figure 9**).

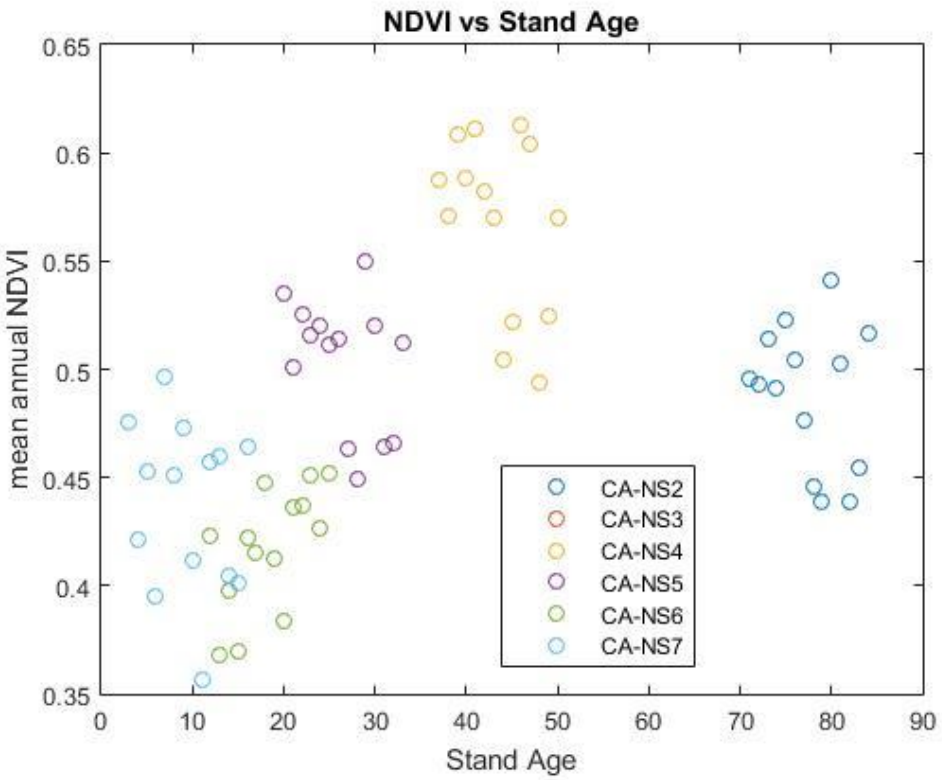

FIGURE 9 - NDVI(MEAN ANNUAL ORIGINAL VALUES) VS STAND AGE

Although the general pattern is similar to the above FPAR and LAI patterns, there are two key differences that are worth mentioning: 1) a reduction in NDVI around 20 years and 2) also a lower NDVI at maturity (80 years) compared to NDVI at 40-50 years old stands. It is difficult to realize whether these results reflect an age-related decline in CA-NS6, or just a site level difference; and whether the reduction of NDVI in CA-NS2 reflects a maturity signal that is unseen by FPAR or LAI, a local bias in the retrieval algorithm, or a true age-related decline.

3.2.1 AGE RELATED CHANGES IN GPP FLUXES

How does Stand age affects the GPP flux? **Figure 10** shows the mean annual GPP for the Canadian sites in relation to the stand age.

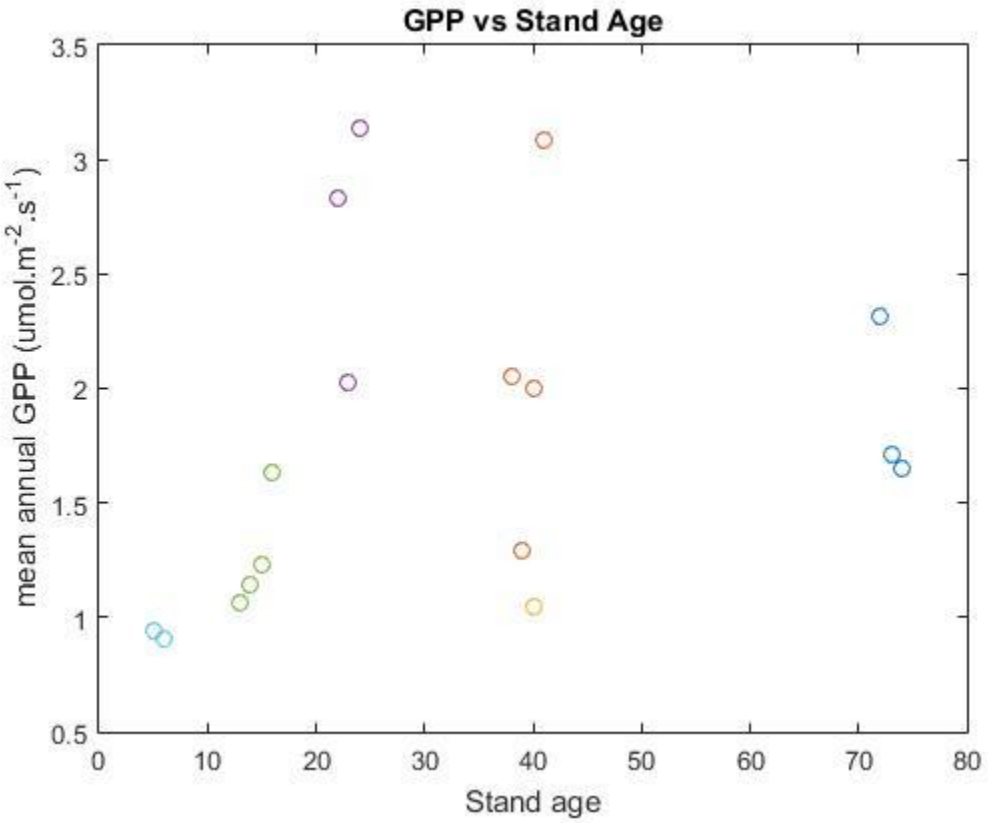

FIGURE 10 - GPP VS STAND AGE

There seems to be a relation between GPP with age, shown in **Figure 10**, but more noise given inter annual variability in other environmental variables (temperature, precipitation), although the upper envelope of GPP seems to follow a stand-driven pattern with a higher GPP in most cases between 20 and 40 years of age, followed by a decline and stability towards the mature 70-80 years old forest. This needs to be confirmed with further research (see **section 4**).

An interesting question arises from the age related changes in GPP and FPAR: whether it is observable an age-related change in ecosystem LUE (light use efficiency) (equation 1)? For that mean annual values where compared and plotted (**figure 11**).

$$LUE = \frac{GPP}{FPAR * Rad} \qquad (1)$$

Where GPP is gross primary production, FPAR is fraction of photosynthetic absorbed radiation and Rad is on radiation intensity.

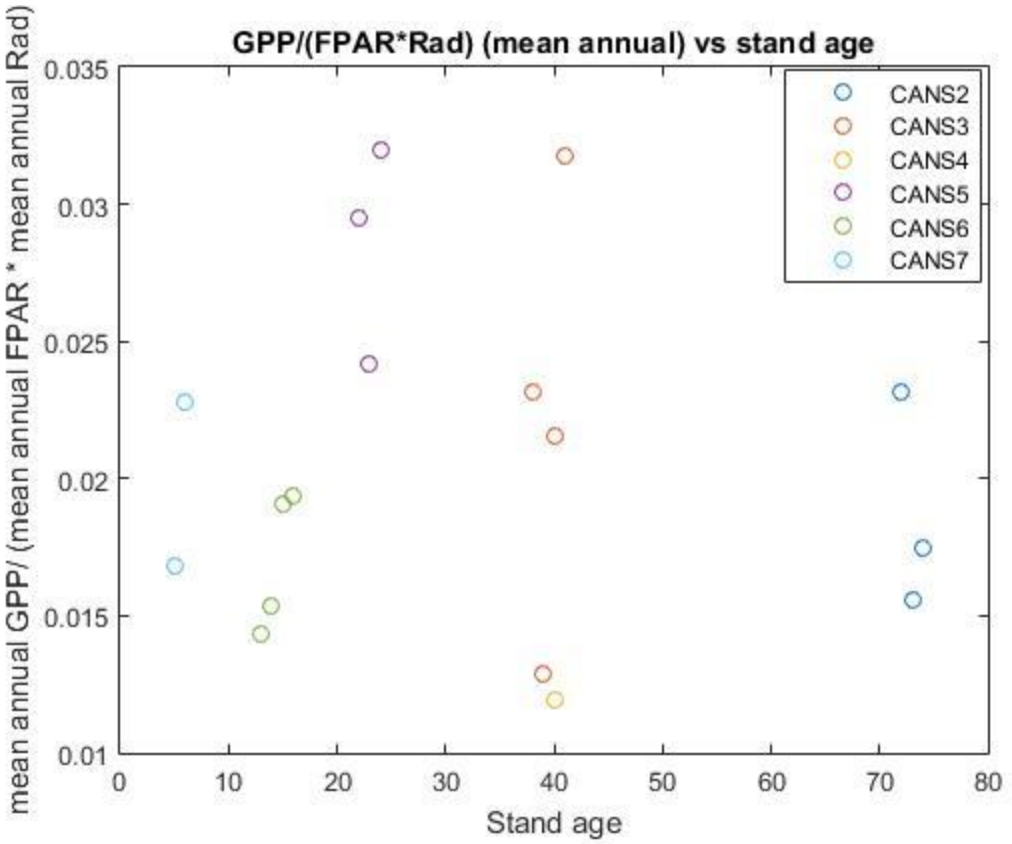

FIGURE 11 -LUE (UMOL/W) VS AGE OF STANDS

Figure 11 shows no obvious relation between LUE and stand age. Hypothetically, there seems to be a pattern in the upper values per site, and maximum LUE could be dependent on age but less optimal temperature and/or water availability conditions would impose the departures from the maximum realizable GPP(see Chasmer et al., 2008).This is something that would be worth further research, and will be discussed in the following section.

4. FUTURE COLLABORATION WITH THE HOST INSTITUTION

Future collaboration with the host institution is foreseen on two papers that the applicant is/will be working on for his PhD thesis at the University of Aveiro. The first concerns vegetation recovery following single vs. recurrent wildfires in maritime pine stands in north-central Portugal and, in particular, the presence of early warning signs of fire-induced tipping-points, with the MODIS-based vegetation proxies applied during this STSM being complementary to the TM- and UAV-based vegetation proxies that were originally foreseen. The second concerns the flux tower measurements foreseen in the FIRE-C-BUDs project during the initial stage of post-fire ecosystem recovery, providing monthly and seasonal estimates of GPP that could be used to validate the relationships with MODIS-based vegetation proxies suggested by the results of this STSM. Consequently, this work will have to be continued even after the completion of the STSM period. The next step is to carry out an n-way ANOVA where several factors will be statistically tested for their relevance in the correlations of the VI-method proxies with the GPP. Additionally, including more chronosequences will allow to confirm results and/or propose new hypothesis to age related VI-developments and links to GPP fluxes.

5. FORESEEN PUBLICATIONS/ARTICLES RESULTING FROM THE STSM

While the results obtained during this STSM are only preliminary, given the short duration of the STSM and the somewhat limited background of the applicant in the methodologies that were applied during the STSM, they are sufficiently promising to justify further work, with the final objective to report them in an international peer-reviewed journal. Since such a publication could be integrated in the applicant's PhD thesis, he is committed to further the work after the end of the STSM and has, in fact, carried on the work after his return to the sending institution.

6. REFERENCES

Baldocchi, D. (2008). TURNER REVIEW No . 15 Breathing of the terrestrial biosphere : lessons learned from a global network of carbon dioxide flux measurement systems, (15), 1–26.

Baldocchi, D. D. (2003). Assessing the eddy covariance technique for evaluating carbon dioxide exchange rates of ecosystems : past , present and future, (November 2002), 479–492.

Carvalhais, N., Reichstein, M., Seixas, J., Collatz, G. J., Pereira, J. S., Berbigier, P., … Valentini, R. (2008). Implications of the carbon cycle steady state assumption for biogeochemical modeling performance and inverse parameter retrieval. *Global Biogeochemical Cycles*, *22*(2), n/a-n/a. https://doi.org/10.1029/2007GB003033

Chasmer, L., McCaughey, H., Barr, A., Black, A., Shashkov, A., Treitz, P., & Zha, T. (2008). Investigating light-use efficiency across a jack pine chronosequence during dry and wet years. *Tree Physiology*, *28*(9), 1395–1406. https://doi.org/10.1093/treephys/28.9.1395

Chen, J., Jönsson, P., Tamura, M., Gu, Z., Matsushita, B., & Eklundh, L. (2004). A simple method for reconstructing a high-quality NDVI time-series data set based on the Savitzky–Golay filter. *Remote Sensing of Environment*, *91*(3), 332–344. https://doi.org/10.1016/j.rse.2004.03.014

Goulden, M. L., Winston, G. C., McMillan, A. M. S., Litvak, M. E., Read, E. L., Rocha, A. V., & Elliot, R. J. (2006). An eddy covariance mesonet to measure the effect of forest age on land-atmosphere exchange. *Global Change Biology*, *12*(11), 2146–2162. https://doi.org/10.1111/j.1365-2486.2006.01251.x

Huete, A. (1997). A comparison of vegetation indices over a global set of TM images for EOS-MODIS. *Remote Sensing of Environment*, *59*(3), 440–451. https://doi.org/10.1016/S0034-4257(96)00112-5

Huete, A., Didan, K., Miura, T., Rodriguez, E. ., Gao, X., & Ferreira, L. . (2002). Overview of the radiometric and biophysical performance of the MODIS vegetation indices. *Remote Sensing of Environment*, *83*(1), 195–213. https://doi.org/10.1016/S0034-4257(02)00096-2

Joiner, J., Guanter, L., Lindstrot, R., Voigt, M., Vasilkov, a P., Middleton, E. M., … Frankenberg, C. (2013). Global monitoring of terrestrial chlorophyll fluorescence from moderate spectral resolution near-infrared satellite measurements: methodology, simulations, and application to GOME-2. *Atmospheric Measurement Techniques Discussions*, *6*(2), 3883–3930. https://doi.org/10.5194/amtd-6-3883-2013

Jönsson, P., & Eklundh, L. (2004). TIMESAT—a program for analyzing time-series of satellite sensor data. *Computers & Geosciences*, *30*(8), 833–845. https://doi.org/10.1016/j.cageo.2004.05.006

Justice, C. ., Townshend, J. R. ., Vermote, E. ., Masuoka, E., Wolfe, R. ., Saleous, N., … Morisette, J. . (2002). An overview of MODIS Land data processing and product status. *Remote Sensing of Environment*, *83*(1), 3–15. https://doi.org/10.1016/S0034-4257(02)00084-6

Knyazikhin, Y., Martonchik, J. V., Diner, D. J., Myneni, R. B., Verstraete, M., Pinty, B., & Gobron, N. (1998). Estimation of vegetation canopy leaf area index and fraction of absorbed photosynthetically active radiation from atmosphere-corrected MISR data. *Journal of Geophysical Research: Atmospheres*, *103*(D24), 32239–32256. https://doi.org/10.1029/98JD02461

Knyazikhin, Y., Martonchik, J. V., Myneni, R. B., Diner, D. J., & Running, S. W. (1998). Synergistic algorithm for estimating vegetation canopy leaf area index and fraction of absorbed photosynthetically active radiation from MODIS and MISR data. *Journal of Geophysical Research: Atmospheres*, *103*(D24), 32257–32275. https://doi.org/10.1029/98JD02462

Rouse, J. W., Hass, R. H., Schell, J. A., & Deering, D. W. (1974). *Monitoring vegetation systems in the great plains with ERTS. Third Earth Resources Technology Satellite (ERTS) symposium* (Vol. 1). https://doi.org/citeulike-article-id:12009708

Sellers, P. J., Los, S. O., Tucker, C. J., Justice, C. O., Dazlich, D. A., Collatz, G. J., & Randall, D. A. (1996). A revised

land surface parameterization (SiB2) for atmospheric GCMs. Part II: The generation of global fields of terrestrial biophysical parameters from satellite data. *Journal of Climate*, *9*(4).

Serbin, S. P., Ahl, D. E., & Gower, S. T. (2013). Spatial and temporal validation of the MODIS LAI and FPAR products across a boreal forest wildfire chronosequence. *Remote Sensing of Environment*, *133*, 71–84. https://doi.org/10.1016/j.rse.2013.01.022

Viovy, N., Arino, O., & Belward, A. S. (1992). The best index slope extraction (Bise): A method for reducing noise in NDVI time-series. *International Journal of Remote Sensing*, *13*(8). https://doi.org/10.1080/01431169208904212

Apendix A

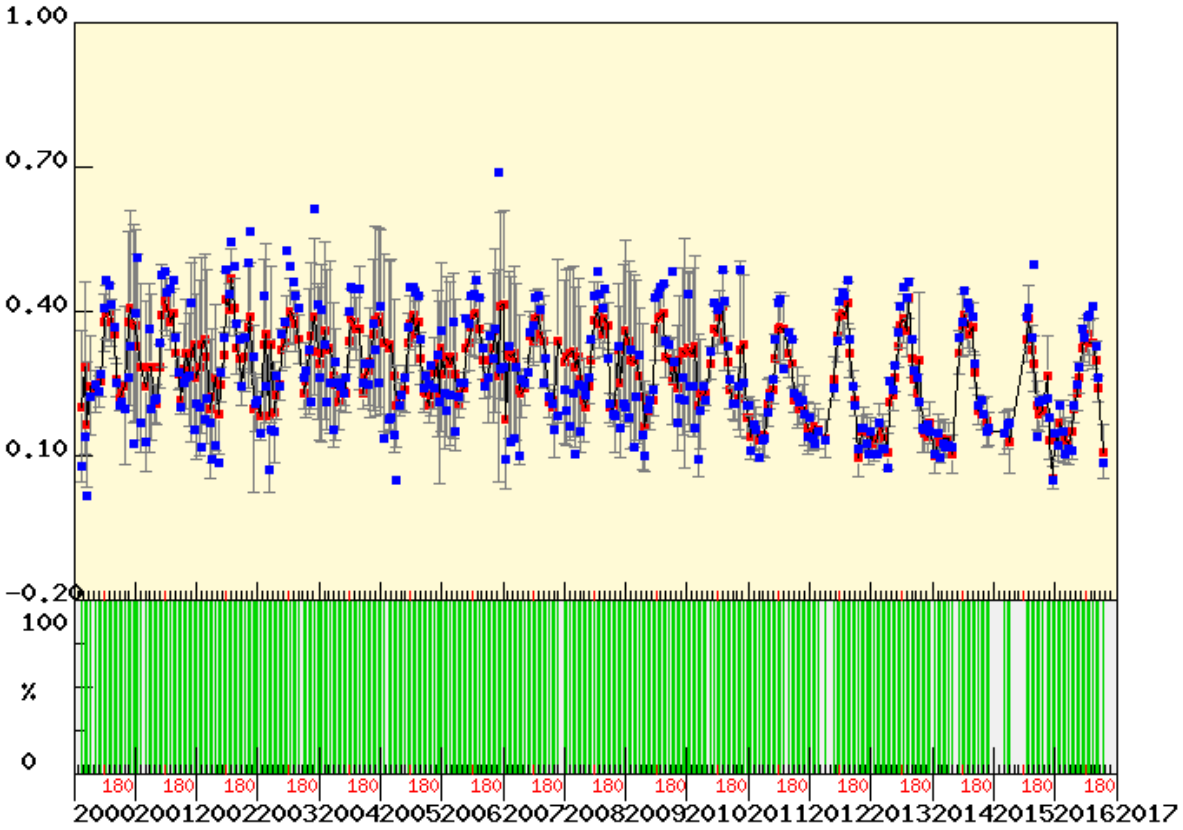

FIGURE 12- EVI TIME SERIES AT CA-NS

Apendix B

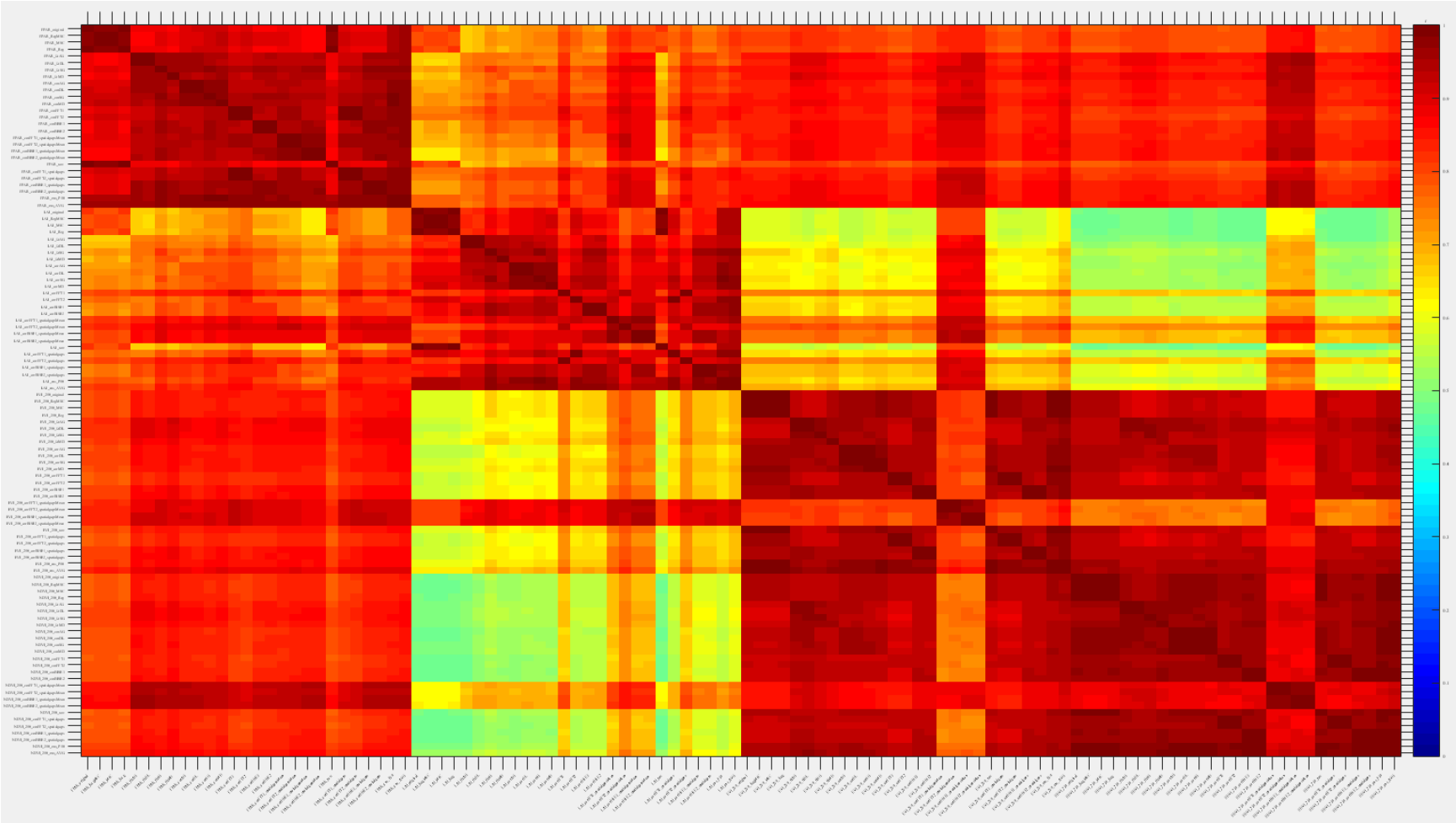

FIGURE 13 - CORRELATIO MATRIX OF PT-MI1 PORTUGAL, ÉVORA